Peierls instability in carbon nanotubes: A first-principles study

Guillaume Dumont,[1] Paul Boulanger,[1] Michel Côté,[1,*] and Matthias Ernzerhof[2]
[1]*Département de physique et Regroupement québécois sur les matériaux de pointe (RQMP), Université de Montréal, C. P. 6128 Succursale Centre-ville, Montréal (Québec), H3C 3J7 Canada*
[2]*Département de chimie, Université de Montréal, C. P. 6128 Succursale Centre-ville, Montréal (Québec), H3C 3J7 Canada*
(Received 19 May 2010; published 15 July 2010)

We present a first-principles study of Peierls distortions in *trans*-polyacetylene, polyacene, and armchair (n,n) carbon nanotubes. Our findings suggest that the ground-state geometries of armchair (n,n) carbon nanotubes, with n up to 6, exhibit a Peierls distortion as it is found for *trans*-polyactetylene. In contrast to previous studies in which no Peierls distortion is found with conventional local and semilocal density functionals, we use a hybrid functional whose exact-exchange admixture has been specifically optimized for the problem at hand.

DOI: 10.1103/PhysRevB.82.035419 PACS number(s): 73.63.Fg, 71.15.Mb, 72.15.Nj, 78.67.Ch

I. INTRODUCTION

The debate whether carbon nanotubes should exhibit a Peierls instability arose shortly after their discovery.[1] *Trans*-polyacetylene (*t*-PA) is the classic example of Peierls instability and since (n,n) armchair nanotubes can be considered as a parallel arrangement of polyacetylene chains along the tube axis, it is natural to suspect that such a deformation is also possible in these systems. Studies[1–3] of the electron-phonon coupling using model Hamiltonians predict a Peierls transition with low critical temperature. Whereas earlier investigations based on density-functional theory (DFT) found a symmetric geometry, more recent investigations using denser grids or refined zone-folding techniques[4–6] also reveal a Peierls instability for small nanotubes. All these studies found an instability at $q=2k_F$, which results in a reduction of the translational symmetry. The corresponding distortion is quite different than the deformation in *t*-PA because at least three unit cells are required to describe it. According to Ref. 5, many more unit cell could be necessary, because they find k_F to be incommensurate with the unit cell. The phonon spectrum obtained with DFT calculations[4–6] also indicates a softening at $q=0$, which corresponds to a deformation that fits into a single unit cell, i.e., a deformation that is quite similar to the one found in *t*-PA.

However, it has been shown[7,8] that the standard local density (LDA) and generalized gradient approximations (GGAs) are unable to reproduce the experimental geometry of trans-polyacetylene,[9–12] underestimating the bond length alternation (BLA) by 70%–80%. Thus, in order to reproduce the correct ground state of *t*-PA from a first-principles method, theories which treat exchange and correlation more accurately have to be employed.[13–15] Hybrid functionals, in which a part of the approximate DFT exchange is replaced by exact exchange, have proven to give a more accurate estimate of the BLA in *trans*-polyacetylene.[13]

The previous DFT studies mentioned above used local and semilocal density functionals but in light of results for *t*-PA, it seems important to consider the effects of hybrid functionals on armchair carbon nanotubes. Notably, it could change the relative strength of the instability at $q=0$ compared to $q=2k_F$. Understanding the nature of the instability is crucial since it could well be related to the superconductivity of small carbon nanotubes in nanopores of zeolites.[16,17] It must be emphasized that extremely small nanotubes, such as the ones explored in this paper, have been synthesized in such pores or are found as the inner tube of double-wall carbon nanotubes.[18] In this paper, we report an *ab initio* study of Peierls instabilities in *trans*-polyacetylene, polyacene (PAc), and (n,n) armchair carbon nanotubes and highlight the importance of including exact exchange in the functional to obtain a dimerized structure.

II. METHOD

All calculations were done with the Kohn-Sham approach of DFT using Gaussian basis sets, as implemented in the periodic boundary conditions (PBC) module of the GAUSSIAN03 package.[19] We employed the 6–311G and 6–31G basis sets for the polymers and the nanotubes respectively, and the Brillouin zones were sampled with over 200 **k** points. Atomic positions and unit cell lengths of the tubes and polymers have been optimized. Several exchange-correlation functionals have been put to work in this study, namely the PBE,[20] B3LYP,[21,22] and HSE,[23] as well as the PBE hybrid,[24] referred thereafter as hPBE, and a generalization of the latter:

$$E_{XC} = (1-x)\Delta E_X^{\mathrm{PBE}} + xE_X^{\mathrm{exact}} + E_C^{\mathrm{PBE}}, \qquad (1)$$

where x is the fraction of exact exchange included in the functional. The PBE and hPBE functionals correspond to $x=0$ and $x=0.25$, respectively. We will refer, hereafter, to the various flavors of this functional by specifying only the fraction of exact exchange x. We would like to stress that the optimal amount of exact exchange mixing depends on the system of interest.[25,26] Therefore, the "best" hybrid functional for the problem at hand contains an unknown parameter. Furthermore we should mention that the implementation of the hybrid methods in the GAUSSIAN03 does not strictly adhere to the Kohn-Sham approach since the nonlocal Hartree-Fock exchange operator is employed instead of the local exchange potential. Experience indicates that this modification has essentially no effect on the predicted ground-state properties.[27] The HSE functional used in this study includes 25% of screened exact exchange and the Cou-

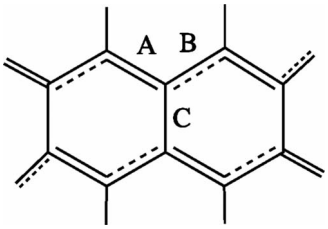

FIG. 1. Most stable configurations obtained for PAc and (n,n) CNTs with $x>0$. Here the double, aromatic and single bonds notation is used to emphasize that the bond lengths are ordered as follows $A<B<C$.

lomb interaction is screened at a distance of 3.5 Å (see the reference by Heyd *et al.*[23] for details of the implementation).

III. RESULTS

Distortion vs exact exchange: In this section, we report the bond length alternation along the system axis, defined as the difference between the long B and short A bonds, and the associated band gap obtained using different exchange-correlation functionals. The systems considered are *trans*-polyacetylene, polyacene, and carbon nanotubes. The distortion found to be the most stable in PAc and (n,n) tubes is depicted in Fig. 1. These systems are very similar to that of a parallel arrangement of distorted *t*-PA chains along the tube (or polymer) axis. The BLA of neighboring chains exhibits a phase difference corresponding to half a cell. Hence, the distorted geometry is found to be a Kekulé-type structure, the bond lengths being all different and are ordered as follows: $A<B<C$ (see Table II). Note that it is also different from what was reported in,[5] but it is very similar to that of[1] and the one found in,[28] which also found a Kekulé-type structure.

Table I shows the BLA (denoted by Δa) and the band gap, E_g, obtained with the B3LYP (20% of E_X^{exact}), hPBE (25% of E_X^{exact}) and HSE (25% of screened E_X^{exact}) functionals for *t*-PA, PAc and the (3,3) nanotube. As expected, the band gap is proportional to the amount of exact exchange included in the functional and so is the BLA. This stems from the fact that Hartree-Fock theory tends to overestimate band gaps and over localize electrons. Hence, an appropriate choice of the parameter x can recover the correct BLA. We see from Table I that although the HSE functional yields a dimerized structure for *t*-PA and PAc, the magnitude of the BLA is less than that obtained with functionals which include the full

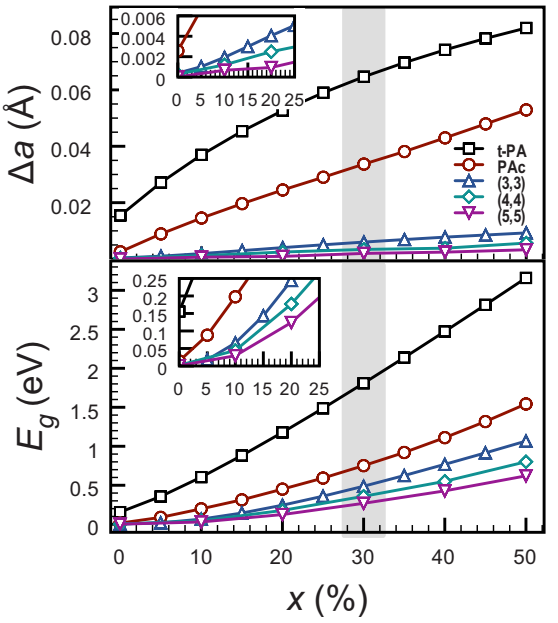

FIG. 2. (Color online) Dimerization amplitude (top panel) and band gap (bottom panel) as a function of the percentage of exact exchange (x) included in the functional. The shaded area indicates the range of x yielding the best agreement between calculated and experimental *t*-PA bond lengths. The insets zoom in on the small-x region.

extent of the exchange interaction suggesting that the medium to long-range exchange interaction increases the dimerization in these systems. In particular, for the (3,3) nanotube, HSE predicts a symmetric geometry with a very small gap. The importance of this long-range interaction could explain the failure of purely local- and semi-local functionals, such as LDA and PBE.

To systematically study the exact exchange dependence of the dimerization amplitude and band gap, we used the functional of Eq. (1) and varied x between 0 and 0.5. Figure 2 shows the dimerization amplitude (top panel) and the band gap (bottom panel) of *t*-PA, PAc, and (n,n) CNTs, for n ranging from 3 to 5, as a function of x. The geometries were optimized for each value of x. The reported band gaps are differences in Kohn-Sham eigenvalues and should be treated only as indications of a trend since the electron-hole interaction is not included and it has been shown to be important in nanotubes.[29,30] The BLA in the tubes scales linearly with the amount of exact exchange, while the band gap follows a

TABLE I. Calculated distortions and band gaps for *t*-PA, PAc, and a (3,3) tube with different exchange-correlation functionals.

	B3LYP		hPBE		HSE	
	Δa (10^{-3} Å)	E_g (eV)	Δa (10^{-3} Å)	E_g (eV)	Δa (10^{-3} Å)	E_g (eV)
t-PA	56.4	1.23	59.0	1.49	49.6	0.84
PAc	24.8	0.44	26.7	0.55	17.0	0.17
(3,3)	4.13	0.25	4.97	0.36	0.0	0.05

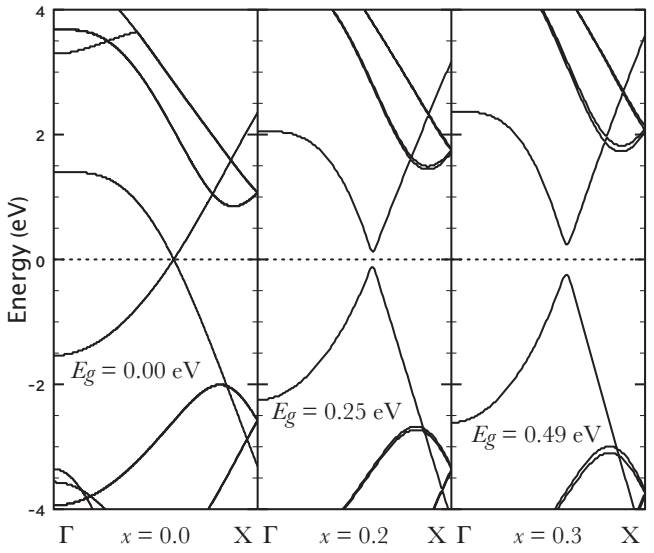

FIG. 3. Bands structures of (3,3) tube for increasing exact exchange mixing; from left to right x takes the values 0.0, 0.2, and 0.3.

power law x^m with $m>1$. This figure also shows that the density only PBE ($x=0$) functional is unable to reproduce the experimental BLA of 0.08 Å nor the band gap of 1.5 eV[31,32] of *trans*-polyacetylene and predicts all (n,n) CNTs to be metallic. The increase in the band gap as a function x is caused by the addition of exact exchange included in the functional and by the geometry of the tube that is more dimerized as x increased.

Figure 3 shows the band structures of a (3,3) tube for $x=0$, 0.2 and 0.3. When no exact exchange is included, $x=0$, the nanotube is metallic. With 30% of exact exchange, the gap obtained is 0.49 eV. It can be seen that the inclusion of exact exchange not only increases the band gap but also stretches the band structure. In particular, the energy differences between van Hove singularities in the density of states widens as the percentage of exact exchange is increased.

A. Optimized geometry of the tubes

To study the Peierls mechanism in more detail, we use the amount of exact exchange that best describes the *trans*-polyacetylene ground state geometry since the tubes and PAc can be viewed as an arrangement of *t*-PA chains. For *t*-PA the best agreement with the experimental geometry was obtained for $x=0.3$. We prefer this hybrid functional over the B3LYP (or a generalization of it) because it recovers the homogenous electron gas limit. In Table II, the optimized bond lengths, differences in total energy with respect to the symmetrical case and the band gaps are reported for *t*-PA, PAc, and (n,n) obtained with $x=0.3$. From these results it is clear that the distortion becomes less significant as the tube diameter increases. Also, all bond lengths seem to converge to the same value of 1.421 Å which corresponds to the hPBE($x=0.3$) value for the C–C bond length in graphene.

The stability of these deformations was evaluated by calculating the total energy gain achieved by deforming the tube. The undistorted geometry was chosen such that it has equal A and B bond lengths, a common feature of aromatic systems. Note that within LDA and PBE, armchair carbon nanotubes also exhibit equal bond lengths. The structure was permitted to relax, under the above mention condition (A=B). This undistorted structure reaches its lowest total energy state when $A^{(0)}=B^{(0)}=\text{mean}(A^{(per)},B^{(per)})$. The bond-length C was allowed to relax but it was found to remain the same as in the fully optimized structure shown in Table II, i.e., $C>A=B$. We calculated the total energy difference per unit cell, ΔE_{tot}, between the distorted and undistorted structures for all tubes. We report the results of this analysis in Table II. As expected, the stability of the deformations decreases rapidly with increasing tube diameter. Using these energy differences as an estimation of the temperature at which the Peierls deformation would occur, we find that it corresponds to a few kelvins for the nanotubes.[33]

To our knowledge, the Peierls distortion in carbon nanotubes has never been directly and conclusively observed in experimental data, owing much from the fact that most readily available nanotubes are larger then the one studied here. As we have shown, the stability of such distortions decreases rapidly with increasing tube diameter. As such, it is comprehensible that small perturbations are enough to wash out this effect. Nonetheless, our results seems to concur with the resistance measurements of Shea *et al.*,[34] which found a sharp increase in resistance at $T=0.8K$ for a bundle of tubes. The diameter of the most abundant nanotube in the sample was 1.4 nm, corresponding to a (10,10) tube. A similar band gap opening, below $T<20$ K, was seen in ^{13}C isotope enriched inner walls in double-wall carbon nanotubes using ^{13}C

TABLE II. Optimized geometries of *t*-PA, PAc and (n,n) CNTs with $x=0.3$.

	Bond lengths (Å)			ΔE_{tot} (meV)	$E_g^{A<B}$ (eV)
	A	B	C		
t-PA	1.361	1.426		27.11	1.66
PAc	1.383	1.416	1.460	15.46	0.749
$n=3$	1.426	1.432	1.440	3.41	0.49
$n=4$	1.423	1.426	1.431	2.10	0.36
$n=5$	1.422	1.424	1.427	1.14	0.27
$n=6$	1.421	1.423	1.424	0.69	0.23

nuclear magnetic resonance.[18] The diameter of these inner tubes was 0.7 nm, corresponding to a (5,5) tube. The radius dependence of the critical temperature and stability of the deformation seems to be corroborated.

B. Connection with the response function

Within linear response theory, the Peierls instability can be understood as a pole in the response function $\chi(r,r')$ or equivalently as a zero eigenvalue in the $\chi^{-1}(r,r')$ spectrum. In a DFT approach, the real response of the system is related to the response function of the noninteracting Kohn-Sham system denoted by $\chi^s(r,r')$ by the following relation:

$$\frac{1}{\chi(r,r')} = \frac{1}{\chi^s(r,r')} - \left[\frac{1}{|r-r'|} + f_{xc}(r,r')\right], \tag{2}$$

where $f_{xc}(r,r')$ is the exchange-correlation kernel. For a one-dimensional (1D) system, the Kohn-Sham non-interacting electron system exhibit a Peierls instability at a wave vector $q=2k_F$. The Coulomb part of the previous equation has a negative contribution. Since the response function $\chi^s(r,r')$ is negative definite, this Coulomb part will make the spectrum of $\chi(r,r')$ more negative. Hence, it tends to decrease any instabilities in Kohn-Sham noninteracting electron system. On the other hand, the exchange-correlation kernel, since it is always negative, should attenuate/cancel the Coulomb part and preserve the Peierls instability. Therefore, the exchange-correlation kernel should contain a long-range contribution of the form $-\frac{\alpha}{q^2}$, where α is a material dependent parameter. We note that a kernel of the form $\chi(q)=-\frac{\alpha}{q^2}$ has been suggested for TDDFT (time-dependent density-functional theory) calculations in order to obtain correct optical spectra.[35] Here, we find that such response functions are important for the ground-state geometry in the system studied in this paper.

Based on this discussion, it is not surprising that exact exchange helps to reestablish the Peierls instability. Essentially, the direct Coulomb interaction alone would diminish the Peierls instability since it would tend to limit the localization of electrons in a same region. The local and near local functionals (LDA, PBE, and HSE) tend to a constant has $q \rightarrow 0$. Hence, they fail to produce an appreciable Peierls distortion as they cannot cancel the Coulomb contribution. The inclusion of some exact-exchange restores a correct long-wave dependence of the kernel. The amount of exact-exchange must be chosen as to give the correct α parameter, which unfortunately will depend on the system studied. In this paper, we suggest that 30% of exact-exchange is nominal for the study of 1D conjugated carbon systems such as *t*-PA, PAc and armchair nanotubes.

IV. CONCLUSIONS

Our DFT calculations show that hybrid functionals are better suited for the description of the properties of *trans*-polyacetylene than local- or semi-local functionals (LDA or GGAs), and hence could be more appropriate to describe the geometry of carbon nanotubes. Using a hybrid functional derived from PBE, we showed that the distortion amplitude and the band gap increases with the amount of exact exchange included in the functional. Using the value of x that best describes the *t*-PA geometry, we found that small radius *armchair* nanotubes should exhibit small lattice distortions that decrease with increasing tube diameter. This deformation should be visible in the absorption spectra of pristine narrow armchair nanotubes, as found in zeolites, as the occurrence of an absorption edge. It should also be visible in the Raman spectra, as a phonon softening and quenching of the Fano line shape at low temperatures. Our particular choice of functional appears appropriate since it recovers the graphene bond lengths for larger tubes, in addition to describing the bond length alternation in *t*-PA correctly.

ACKNOWLEDGMENTS

We would like to thank Richard Martel for helpful discussions and his assistance and Jeffrey Frey for providing the TubeGen Utility. Financial support through FQRNT and NSERC as well as computational resources made available by the Réseau québécois de calcul de haute performance (RQCHP) are gratefully acknowledged.

*michel.cote@umontreal.ca

[1] J. W. Mintmire, B. I. Dunlap, and C. T. White, Phys. Rev. Lett. **68**, 631 (1992).
[2] Y. Huang, M. Okada, K. Tanaka, and T. Yamabe, Solid State Commun. **97**, 303 (1996).
[3] A. Sédéki, L. G. Caron, and C. Bourbonnais, Phys. Rev. B **62**, 6975 (2000).
[4] K.-P. Bohnen, R. Heid, H. J. Liu, and C. T. Chan, Phys. Rev. Lett. **93**, 245501 (2004).
[5] D. Connétable, G.-M. Rignanese, J.-C. Charlier, and X. Blase, Phys. Rev. Lett. **94**, 015503 (2005).
[6] S. Piscanec, M. Lazzeri, J. Robertson, A. C. Ferrari, and F. Mauri, Phys. Rev. B **75**, 035427 (2007).
[7] J. W. Mintmire and C. T. White, Phys. Rev. B **35**, 4180 (1987).
[8] J. Paloheimo and J. von Boehm, Phys. Rev. B **46**, 4304 (1992).
[9] C. R. Fincher, C. E. Chen, A. J. Heeger, A. G. MacDiarmid, and J. B. Hastings, Phys. Rev. Lett. **48**, 100 (1982).
[10] C. S. Yannoni and T. C. Clarke, Phys. Rev. Lett. **51**, 1191 (1983).
[11] H. Kahlert, O. Leitner, and G. Leising, Synth. Met. **17**, 467 (1987).
[12] Q. Zhu and J. E. Fisher, Solid State Commun. **83**, 179 (1992).
[13] S. Suhai, Phys. Rev. B **51**, 16553 (1995).
[14] C. H. Choi, M. Kertesz, and A. Karpfen, J. Chem. Phys. **107**, 6712 (1997).
[15] C. H. Choi and M. Kertesz, J. Chem. Phys. **108**, 6681 (1998).
[16] Z. Tang, L. Zhang, N. Wang, X. Zhang, G. Wen, G. Li, J. Wang, C. Chan, and P. Sheng, Science **292**, 2462 (2001).

[17] I. Takesue, J. Haruyama, N. Kobayashi, S. Chiashi, S. Maruyama, T. Sugai, and H. Shinohara, Phys. Rev. Lett. **96**, 057001 (2006).

[18] P. M. Singer, P. Wzietek, H. Alloul, F. Simon, and H. Kuzmany, Phys. Rev. Lett. **95**, 236403 (2005).

[19] M. J. Frisch, G. W. Trucks, H. B. Schlegel, G. E. Scuseria, M. A. Robb, J. R. Cheeseman, J. A. Montgomery, Jr., T. Vreven, K. N. Kudin, J. C. Burant, J. M. Millam, S. S. Iyengar, J. Tomasi, V. Barone, B. Mennucci, M. Cossi, G. Scalmani, N. Rega, G. A. Petersson, H. Nakatsuji, M. Hada, M. Ehara, K. Toyota, R. Fukuda, J. Hasegawa, M. Ishida, T. Nakajima, Y. Honda, O. Kitao, H. Nakai, M. Klene, X. Li, J. E. Knox, H. P. Hratchian, J. B. Cross, V. Bakken, C. Adamo, J. Jaramillo, R. Gomperts, R. E. Stratmann, O. Yazyev, A. J. Austin, R. Cammi, C. Pomelli, J. W. Ochterski, P. Y. Ayala, K. Morokuma, G. A. Voth, P. Salvador, J. J. Dannenberg, V. G. Zakrzewski, S. Dapprich, A. D. Daniels, M. C. Strain, O. Farkas, D. K. Malick, A. D. Rabuck, K. Raghavachari, J. B. Foresman, J. V. Ortiz, Q. Cui, A. G. Baboul, S. Clifford, J. Cioslowski, B. B. Stefanov, G. Liu, A. Liashenko, P. Piskorz, I. Komaromi, R. L. Martin, D. J. Fox, T. Keith, M. A. Al-Laham, C. Y. Peng, A. Nanayakkara, M. Challacombe, P. M. W. Gill, B. Johnson, W. Chen, M. W. Wong, C. Gonzalez, and J. A. Pople, *Gaussian 03, Revision C.02* (Gaussian, Inc., Wallingford, CT, 2004).

[20] J. P. Perdew, K. Burke, and M. Ernzerhof, Phys. Rev. Lett. **78**, 1396 (1997).

[21] A. Becke, J. Chem. Phys. **98**, 5648 (1993).

[22] P. Stephens, F. Devlin, C. Chabalowski, and M. Frisch, J. Chem. Phys. **98**, 11623 (1994).

[23] J. Heyd, G. E. Scuseria, and M. Ernzerhof, J. Chem. Phys. **118**, 8207 (2003), the functional referred as HSE2PBE in the GAUSSIAN 03 package was used in this study.

[24] J. P. Perdew, K. Burke, and M. Ernzerhof, Phys. Rev. Lett. **77**, 3865 (1996), the hPBE functional includes 20% of exact exchange. This functional is referred as PBE1PBE in the GAUSSIAN 03 package.

[25] M. Ernzerhof, Chem. Phys. Lett. **263**, 499 (1996).

[26] M. Ernzerhof, in *Density Functionals: Theory and Applications, Lecture Notes in Physics*, edited by D. P. Joubert (Springer Verlag, Berlin, 1998), Vol. 500.

[27] A. M. Teale and D. J. Tozer, J. Chem. Phys. **122**, 034101 (2005).

[28] M. T. Figge, M. Mostovoy, and J. Knoester, Phys. Rev. Lett. **86**, 4572 (2001).

[29] C. D. Spataru, S. Ismail-Beigi, L. X. Benedict, and S. G. Louie, Phys. Rev. Lett. **92**, 077402 (2004).

[30] F. Wang, D. J. Cho, B. Kessler, J. Deslippe, P. J. Schuck, S. G. Louie, A. Zettl, T. F. Heinz, and Y. R. Shen, Phys. Rev. Lett. **99**, 227401 (2007).

[31] S. D. Phillips, R. Worland, G. Yu, T. Hagler, R. Freedman, Y. Cao, V. Yoon, J. Chiang, W. C. Walker, and A. J. Heeger, Phys. Rev. B **40**, 9751 (1989).

[32] H. Eckhardt, J. Chem. Phys. **79**, 2085 (1983).

[33] The mean-field expression (Ref. 36) relating the band gap to the critical temperature could not be used since our obtained band gaps do not correspond to those of the model Hamiltonian employed in this formalism.

[34] H. R. Shea, R. Martel, and P. Avouris, Phys. Rev. Lett. **84**, 4441 (2000).

[35] S. Botti, A. Schindlmayr, R. D. Sole, and L. Reining, Rep. Prog. Phys. **70**, 357 (2007).

[36] M. V. Sadovskii, *Diagrammatics, Lectures on Selected Problems in Condensed Matter Theory* (World Scientific, New York, 2006).